ISSN 1330–0008
CODEN FIZAE4

EXPERIMENTAL STUDY OF Ar-O_2 LOW-PRESSURE DISCHARGE

VANJA MARGETIĆ and DAMIR VEŽA

Institute of Physics, P. O. Box 304, HR-10001 Zagreb, Croatia
E-mail: veza@ifs.hr, Tel.: +385-1-4680211

Received 16 March 1998; Accepted 24 June 1998

We report measurements of electron temperature of DC and RF discharge in pure Ar and Ar + 10% O_2 gas mixture, and the measurements of collisional broadening by argon of three oxygen lines at 777 nm (3p $^5P_{0,1,2} \to$ 3s $^5S_2$ transitions) in an Ar + 10% O_2 gas mixture. The electron temperature is determined using the double-probe technique and the logarithmic-plot method. The line widths of oxygen atomic lines broadened by argon were measured with the high-resolution monochromator and later analyzed numerically.

PACS numbers: 32.70.Jz, 33.70.Jg UDC 535.33

Keywords: collisional line broadening of oxygen lines, three oxygen lines at 777 nm, discharge in pure Ar and in Ar + 10% O_2 gas

1. Introduction

Low-pressure noble-gas glow discharges are very frequently subject of both basic and applied research and widely used in industrial technological processes. In most cases argon is used as the working gas. In some applications oxygen is added, but in some other applications the argon plasma must be free of oxygen. It is of interest for successful applications that basic parameters of Ar/O_2 plasma (electron temperature, electron density and energy-distribution function, densities of metastable atoms, atomic-interaction parameters) are investigated. Measurements of basic parameters provide a better understanding of very complex Ar/O_2 plasma processes and they are necessary as input data for computer simulations which are the subject of much recent research [1].

There are numerous examples of basic and applied research which require the knowledge of the basic atomic or plasma parameters for the mixture of argon and oxygen (see Ref. 2 and references therein). Due to its strong oxidation properties, the presence of oxygen may have an enormous impact on the course of the processes in plasma and on the course of the plasma-electrode–surface processes. For example, argon is used as the ignition gas in high-pressure metal-halide and sodium lamps. The presence of oxygen in argon in as small a concentration as 10^{-6} or more, drastically shortens the lamp lifetime [3]. Therefore, it is of great importance not only to study the basic Ar/O_2 processes but also to develop and further improve techniques for detection of small amounts of oxygen in (argon) plasmas [4]. Another huge area of application of the Ar/O_2 plasma is in the microelectronics industry, where it is used as a tool for depositing thin films, and for etching metals and semiconductors. Some recent investigations showed that if deposition of Pt thin films (the highest quality microelectrodes in contemporary microprocessors) is done under precisely controlled conditions in the mixture of Ar with 10% O_2, the defect-free films with desired crystallographic orientation are obtained [5].

In spite of such significance of argon-oxygen discharges for various applications, and of big interest for basic atomic parameters which are necessary for computer plasma modeling, there is still a lack of information on Ar/O_2 plasma parameters in general, and especially on Ar-O^* atomic interaction parameters. The reason for this lies, probably, in the complexity of the low-pressure Ar/O_2 plasma. Even a pure low-pressure argon discharge is a rather complex plasma, comprising electrons, ground state argon atoms, metastable argon atoms, argon ions, Ar_2^* and Ar_2^+ molecules, and impurity atoms existing in argon or sputtered from electrodes [6,7]. The mixed argon-oxygen plasma is much more complicated. Oxygen is an electron attaching gas and it affects properties of argon plasma even at minute O_2 concentrations. The density of metastable argon is very sensitive to any admixture of oxygen [2], but one can expect the change of all other plasma parameters such as electron density (n_e) and electron temperature (T_e), too. Atomic oxygen in the ground state, metastable oxygen atoms, oxygen ions, O_2^* and O_2^+ molecules are generated in the discharge after complicated collisional excitation, dissociation and ionization processes involving molecular and atomic oxygen. The very important result is that the presence of oxygen induces the appearance of different argon-oxygen collision complexes.

There is a strong experimental evidence that the formation of excited atomic oxygen in triplet and quintet atomic states (Fig. 1) follows different excitation, ionization and dissociation pathways, depending on the type of the carrier noble gas [6]. In the case of lighter noble gases (He, Ne), it seems that the Penning ionization of O_2 is the dominating ionization mechanism [8]:

$$\mathrm{He}^* + \mathrm{O}_2 \rightarrow \mathrm{He} + (\mathrm{O}_2^+)^* + \mathrm{e}^- . \tag{1}$$

The excited molecular ions $(O_2^+)^*$, after dissociative recombination, produce excited atomic oxygen, O^*, and ground-state oxygen atoms, $O(2^3P)$:

$$(O_2^+)^* \ + e^- \ \rightarrow O^* + O(2^3P). \tag{2}$$

Excited oxygen, O*, can appear in triplet or quintet states, depending on the excitation and dissociation pathways of O_2 and O_2^+ molecules.

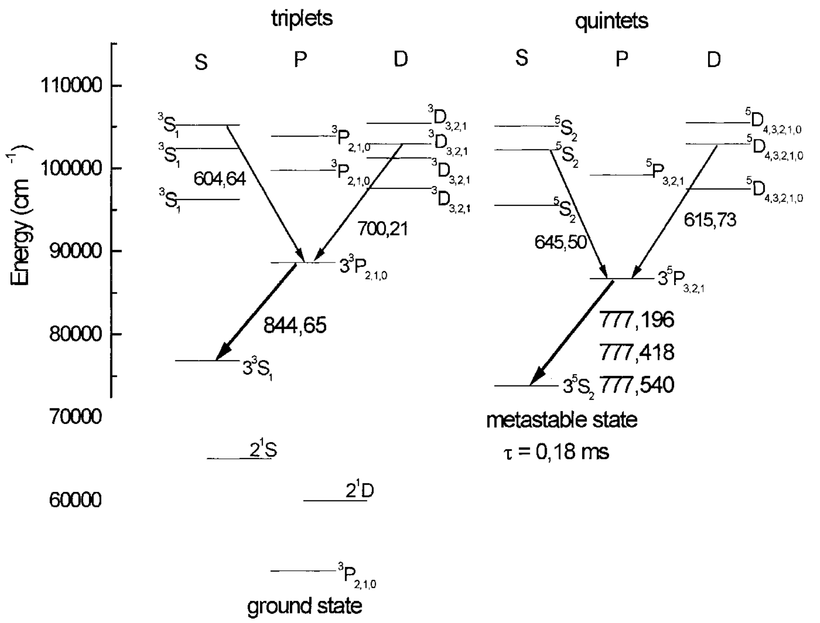

Fig. 1. Term diagram of oxygen.

However, if heavier noble gases (Ar, Kr, Xe) are used, more complicated processes cause excitation, ionization and dissociation of oxygen molecules. The first stage is the formation of an excited complex molecule in collisions of argon metastables and O_2:

$$Ar^* + O_2 \rightarrow (Ar\ O_2)^*. \tag{3}$$

The second stage is dissociation of this complex to argon atoms in the ground state (2^3P) and excited oxygen atoms in 2^1S_0 and 2^1D_2 atomic states [6,9]:

$$(Ar\ O_2)^* \rightarrow Ar + O(2^3P) + O^*(2^1S^0, 2^1D_2) + \Delta E. \tag{4}$$

The energy defect shared by two oxygen atoms, ΔE, contributes to the non-thermal velocity distribution of the involved atomic populations. Atomic populations in 2^1S_0 and 2^1D_2 atomic states ("warm atoms", see Fig. 1), possessing this non-thermal velocity distribution, are transferred to the higher atomic states $O^*(3^3S_0, 3^3P_J)$ by electron-atom collisions [9]. As a consequence, wide and anomalously broadened atomic lines, corresponding to transitions involving these triplet atomic levels, are observed in emission and laser atomic absorption [10]. On the other hand, if higher atomic states are populated through electron-atom collisions from the ground state ("cold atoms"), the thermal velocity distribution is preserved, and the line width reflects Maxwell's velocity distribution. That is exactly the case with oxygen quintet levels 3^5S_2 and 3^5P_J, where the thermal velocity distribution of ground state atoms is preserved in electron excitation processes, resulting in thermal velocity distribution of atomic populations involved in the formation of the 777 nm lines.

In this paper we report the electron temperature measurements of DC and RF discharges in pure Ar and Ar + 10% O_2 mixture, and the measurements of collisional broadening by argon of three oxygen lines at 777 nm (3p $^5P_{0,1,2}$ $\rightarrow$3s $^5S_2$ transitions) in the same gas mixture. It is of interest to compare measurements of electron temperatures (and other related plasma parameters) in pure argon discharge to those in mixed argon-oxygen discharge, as well as the temperatures of DC-excited plasmas to RF-excited ones. Regarding oxygen line broadening, there are some preliminary data on the argon broadening of infrared oxygen lines at 845 nm (3p $^3P_{0,1,2} \rightarrow$ 3s $^3S_1$, [11]). There are several reports on the Doppler-free high resolution measurements of isotope line shift and hyperfine structure of oxygen atomic levels involved in atomic transitions at 777 nm, which are important for possible optical cooling of oxygen atoms (Ref. 12 and references therein). To our knowledge though, there is still no systematic classical or laser measurements of collisional broadening of the 777 nm oxygen lines by argon atoms.

2. *Experiment*

A block diagram of the experimental arrangement used in our measurements of atomic oxygen line broadening and electron temperature is shown in Fig. 2. The line broadening measurements have been performed using a plasma cell, a high resolution monochromator, lock-in detection followed by A/D conversion, and computer data acquisition. The electron temperature measurements have been performed using the same plasma cell, a variable-polarity voltage source and two digital voltmeters to simultaneously measure the probe voltage and the probe current.

The plasma is generated in a 20 cm long cell (Fig. 3), made of Pyrex glass, with the inner diameter of 1.5 cm. Prior to the use in the experiment, the cell was washed with the chromsulfuric acid and distilled water, followed by one-day outgassing at elevated temperature (300 °C) and low cell residual pressure ($< 5{\cdot}10^{-3}$ mbar). Finally, it has been self-cleaned by running a DC discharge in the flow of pure argon (10 mA, 1000 V, 8 hours at 0.5 mbar).

The DC excitation is produced by an unregulated stable high-voltage source (maximum voltage 4 kV, max current 0.1 A, ripple $\approx$ 0.1%). The electrodes were made of stainless steel tubing (type 304) with the inner diameter of 1 cm and 3 cm long. The electrode spacing is 8 cm. Typical currents used here were about 1 - 10 mA (corresponding to current densities of about 0.5 - 5 mA/cm^2).

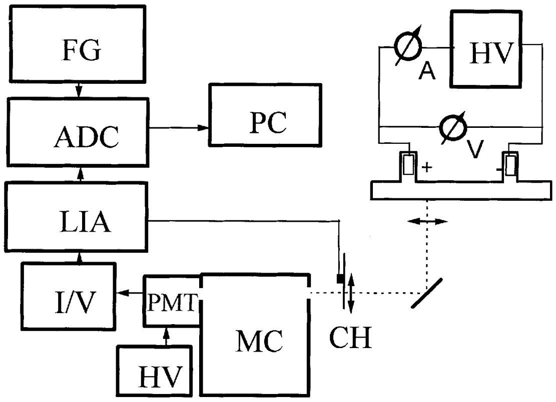

Fig. 2. Experimental arrangement. HV: high voltage source, CH: chopper, MC: monochromator, PMT: photomultiplier tube, I/V: current-to-voltage converter, LIA: lock-in amplifier, ADC: analog-to-digital converter, FG: function generator, V and A: digital volt(amper)-meter.

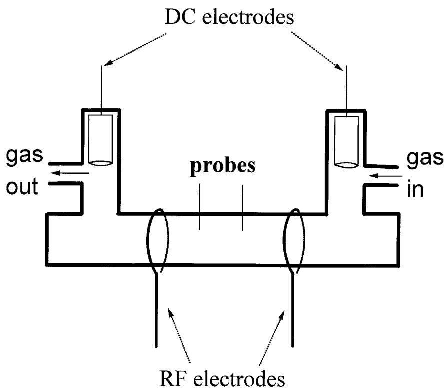

Fig. 3. Discharge cell.

The RF excitation is performed using a homemade 60 MHz RF generator based on a 6360A tetrode tube [13]. Two silvered O-shaped electrodes, made of copper wire (wire diameter 2 mm), embracing the cell and spaced about 6 cm are used for plasma excitation. The amount of RF power delivered to the plasma is not known exactly, but according to the 6360A specifications it cannot be more than several watts.

During the experiment, we run the discharge in a steady flow of gas (pure argon or argon-oxygen mixture) at a flow rate of about 5 cm^3 s^{-1}. The reason is that the oxygen (even in small quantities) in the gas mixture strongly reacts with the surface of electrodes and probes, causing a rather unstable discharge operation if the cell is closed. If the gas mixture flows steadily through the discharge cell, the stream of fresh gas washes the cell, allowing a quiet and stable discharge. The gas we used was the commercial mixture ("Messer Griesheim AG"), containing 10% of naturally abundant molecular oxygen (99.76% $^{16}O_2$, 0.2% $^{18}O_2$, and 0.04% $^{17}O_2$). The gas pressure was monitored continuously by a digital Pirani gauge ("Leybold Thermovac TM20") with an accuracy better than 5%.

3. Results and discussion

3.1. Determination of electron temperature

Regarding the low-temperature plasma characterization, one is concerned with measuring the electron temperature T_e, the electron density n_e, and the electron energy distribution function $f_0(v)$. To this purpose, Langmuir probes have been used for over 70 years [14,15]. It is a well known method to measure important parameters of low-pressure and low-temperature plasmas. In our experiment, two probes made of thin platinum wire (0.4 mm diameter), spaced 2.8 cm and inserted about 0.5 cm perpendicularly into the plasma column have been used for the electron-temperature measurements (Fig. 3). Prior to the measurements, the probes were carefully self-cleaned by running a weak DC discharge in pure argon flowing through the cell under the pressure of 100 Pa (1 mbar). The probe system

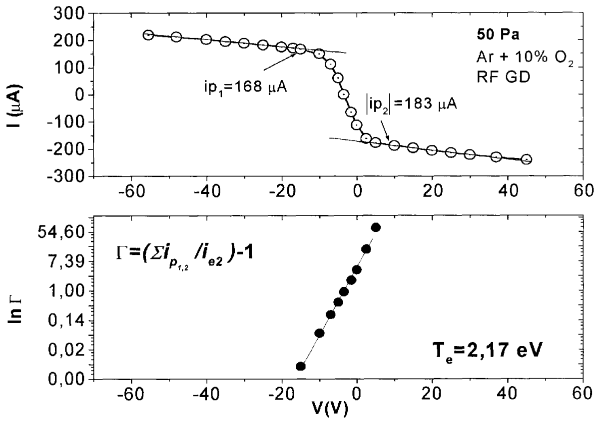

Fig. 4. Typical double-probe characteristic curve (up) and an example of the electron-temperature determination using the logarithmic plot method (down). The temperature is determined from the slope of the $\ln\Gamma$ *versus probe voltage plot.* $i_{p_{1,2}}$ *are positive ion saturation currents to probes 1 and 2, respectively, and* i_{e_2} *is the electron current to probe 2. Typical statistical error of the temperature determination by this method is less than 10%.*

applied in our experiment can be used, in principle, either as a set of single probes or as a double-probe setup [16]. As we were interested in a direct comparison of DC- and RF-driven discharges, we have chosen the double-probe setup for the measurements of the electron temperature. This method is appropriate for the determination of electron temperature even in the absence of a reference electrode, as in the case of an RF-driven discharge.

The double-probe method uses two (identical) Langmuir probes connected to a voltage source of reversible polarity. The probe system is permitted to float. The potential difference between probes is varied from about – 60 V to about + 60 V, and the current-voltage characteristic of the double probe is determined. The electron temperature is determined using the logarithmic plot method [16]. It is based on the Maxwell–Boltzmann distribution of charged particles in plasma potential, plasma sheath properties and Kirchhoff's current law (taking into account electron and positive-ion currents to probes 1 and 2). Figure 4 shows a typical data plot. These data were collected in the case of the RF discharge in Ar + 10% O_2 mixture at the pressure of 50 Pa and a flow rate of about 5 cm^3/s. Maximum current through the double-probe circuit is determined by positive-ion saturation currents ($i_{p_{1,2}}$) to both probes. The asymmetry of the probe characteristics indicates that the probes used in our cell are slightly dissimilar in size and shape, and that they were located at positions characterized by slightly different plasma potential. This, however, doesn't influence the determination of electron temperature since there is a quite simple relation between the parameter Γ, defined as

$$\Gamma = \frac{\sum |i_p|}{i_{e_2}} - 1,$$

and the potential difference between probes V:

$$\ln \Gamma \sim -\frac{e}{kT_e} V.$$

That is, the reciprocal value of the slope of the semi-log plot $\ln \Gamma(V)$ versus V equals the electron temperature in eV.

The pressure range was 50 - 500 Pa (0.5 - 5 mbar). Figures 5a-d show electron temperatures of the DC and the RF discharge. The electron temperature of the DC discharge in pure argon is about 3 eV, and in Ar+10%O_2 mixture it is about 3.3 eV. The electron temperature of the RF discharge in pure argon is about 1.7 eV, and in Ar+10%O_2 mixture it is about 2.3 eV. Although the investigated pressure range is rather small (only one decade) one can see a small increase of the electron temperature with the pressure in the case of the Ar+10%O_2 RF discharge and a small decrease of the electron temperature with the pressure in the case of DC discharge. The DC case is in accordance with other more extensive measurements in Ar+10%O_2 mixture [17]. Generally, with addition of oxygen the increase of electron plasma temperature, accompanied with the decrease of electron density, is observed in other similar experiments with Ar/O_2 mixtures [17,2]. A plausible explanation is that the uniform distribution of O_2 in the discharge spreads electron attachment and electron loss processes, resulting in a uniform decrease of n_e.

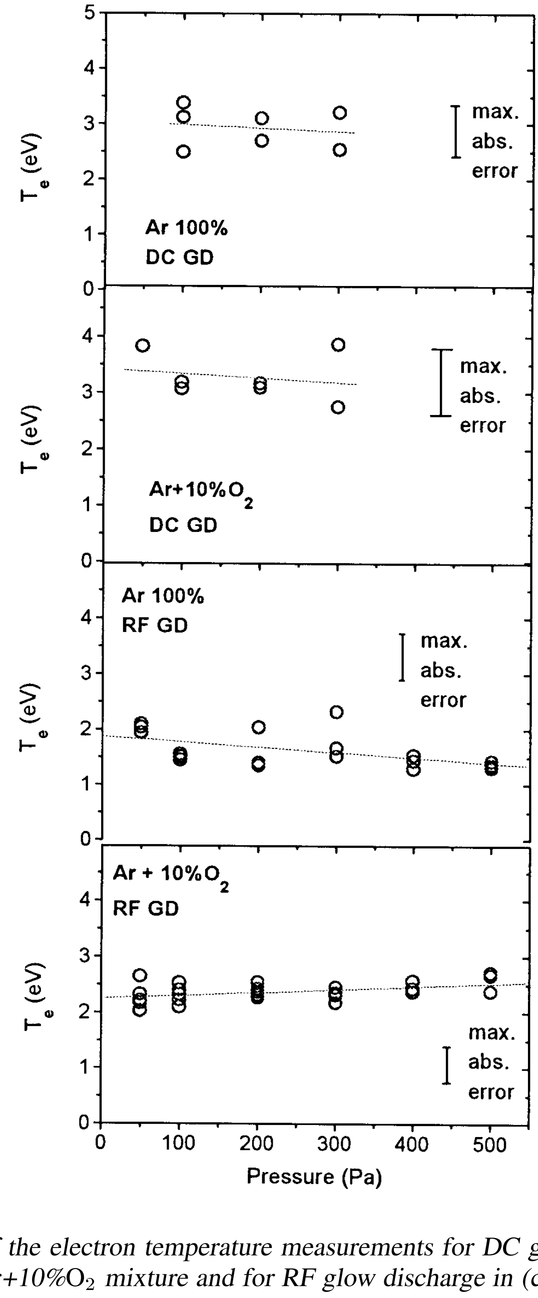

Fig. 5. Results of the electron temperature measurements for DC glow discharge in (a) pure argon, (b) Ar+*10%*O_2 *mixture and for RF glow discharge in (c) pure argon and (d)* Ar+*10%*O_2 *mixture.*

Mass-spectrometry measurements show that the dominant ion in argon plasma is Ar^+ [18]. With addition of oxygen, the O_2^+ density rises on account of Ar^+ [18], until O_2^+ takes the role of the dominant ion. The critical O_2 percentage seems to be about 30% [18]. The decrease of Ar^+ density is caused by quenching of Ar^* by atomic oxygen and O_2 [2], and one can assume that in the Ar/10% O_2 mixture both the O_2^+ and the Ar^+ ions probably play an important role in sustaining the discharge.

3.2. *The line shape of 3p* $^5P_{0,1,2} \rightarrow$ *3s* $^5S_2$ *transitions*

The head of the plasma positive column is being imaged by a standard system of two lenses onto the entrance slit of a high-resolution monochromator ("Jobin Yvon" THR1500, optical system focal length 1.5 m, aperture number 1:10, holographic grating of 2400 g/mm, entrance/exit slit widths fixed to 25 μm, slit height 5 mm). Dispersed light is detected by a photomultiplier (EMI 9558QB), and after lock-in detection (Brookdeal model 401A) fed into the first channel of a 14 bit A/D converter, and finally recorded in a PC. The second channel of the A/D converter is used for acquisition of the reference signal, used for the accurate calibration of the wavelength scale.

Oxygen fluorescence originates from the negative glow region as well as from the positive column of the discharge, but we have chosen the positive column for the line shape studies because of a better long-term signal-to-noise ratio.

We studied the collisional broadening of oxygen transitions at 777 nm (3p $^5P_{0,1,2} \rightarrow$ 3s $^5S_2$) by argon. The pressure dependence has been studied in Ar + 10% O_2 gas mixture in the pressure range 50 - 800 Pa (0.5 - 8 mbar). The resulting line shape is convolution of the monochromator instrumental function, the Doppler profile caused by thermal motion of gas atoms and the Lorentzian function representing the collisional broadening. In principle, besides these three broadening mechanisms, the natural broadening and the oxygen self-broadening also contribute to the measured line width [19]. However, the Doppler broadening, the instrumental broadening and the pressure broadening by argon are the dominant broadening mechanisms resulting in several orders of magnitude larger widths than the other ones.

To analyze these line shapes, we must know very precisely the width and the shape of the instrumental function for our monochromator (FWHM: $\Delta\lambda_I$) and the gas temperature determining the Doppler width of the lines (FWHM: $\Delta\lambda_D$). Accurate tests performed on many spectral lines studied in our laboratory for several years have shown that the "Jobin Yvon" THR1500 monochromator has a pure triangular instrumental function for the slit widths larger then 15 μm, and a nearly diffraction instrumental function for slit widths smaller than 15 μm. However, exact width and shape of the instrumental function must be accurately determined before and in the course of the measurements. To this purpose, we measured (a) isotope and hyperfine structure of the well-known mercury green line at 546.1 nm (from the low-pressure mercury lamp), and (b) the apparent shape and the width of the He–Ne laser line. The monochromator was used in the double-pass mode, enabling ultimate resolution of about $4 \cdot 10^5$ at 546.1 nm for slit widths smaller than 15 μm [20]. A typical determination of monochromator resolution and instrumental function is shown in Fig. 6. It shows the appearance of the He–Ne laser line measured in diffuse laser light. The scanning speed of the monochromator was set to 4 pm/min and the entrance and the exit slit widths were set to 25 μm with slit heights of 5 mm. The corresponding instrumental function is purely triangular with a FWHM of $\Delta\lambda_I = 2.5$ pm and the resolution $R \approx 2.6{\cdot}10^5$ at

632.8 nm. The shape and width of the instrumental function have been checked daily before and after oxygen-line measurements. Daily variations were completely negligible, and weekly variations were within $\pm$ 0.1 pm. From these measurements, we determined the instrumental function of our monochromator as triangular-shaped with $\Delta\lambda_I = (2.5 \pm 0.1)$ pm.

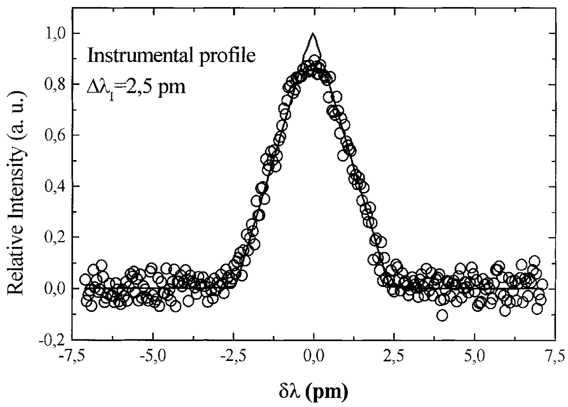

Fig. 6. Instrumental function of the Jobin Yvon THR1500 monochromator.

Another unknown parameter, the gas temperature, has been controlled daily by measuring the Doppler width of the argon line at 811.5 nm and by monitoring the temperature in the laboratory. The Lorentzian width of this argon line has been measured very accurately in laser atomic-absorption experiment [21]. In our experiment, the Doppler width was determined by fitting the experimental line profile to a convolution of the instrumental, Lorentzian and Doppler functions using the Doppler width as the only free parameter. The temperatures obtained from 811.5 nm Ar line Doppler widths were identical to the room temperatures (about 298 K). Actually, the gas is at room temperature in the majority of experiments on the low-pressure discharges. Elevated temperatures of the carrier gas ($T \geq$ 300 K) are measured only in the cases of current densities higher than 50 mA cm^{-2} [7], which is almost two orders of magnitude higher current density than the one used in our experiment.

To avoid any distortion of the instrumental profile, the lines were measured using very low monochromator scanning speeds (2 or 4 pm/min, i.e. 20 to 40 mA/min). The sampling frequency of the A/D conversion was 10 Hz, corresponding to the sampling speed of 0.03 to 0.06 mA/s and the average total number of 2500 (or 5000) data points per line profile. The measured line shape (Fig. 7a,b) is the convolution of the monochromator instrumental function, the Doppler function, and the Lorentzian function representing the pressure broadening by argon atoms. The emission profiles were analyzed using our own multiparameter least squares fitting routine written in "Matlab©" [22]. Of course, the confidence in the fitting procedure and in the single fitted quantity decreases with the number of used parameters, but in our case, the oxygen Lorentzian line width (FWHM: $\Delta\lambda_L^O$) was the only free parameter. The core of the fitting program is constructed using the powerful

"Matlab©" routines *fft.m* and *ifft.m* for the discrete fast Fourier transformation (FFT) and for the inverse FFT, respectively. Generally, the Fourier

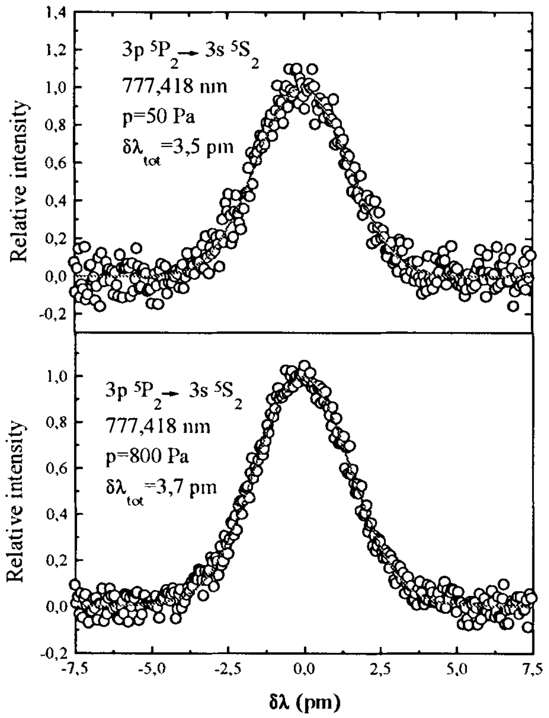

Fig. 7. Typical emission profiles of the 777,418 nm *oxygen line measured at the pressure of (a) 50* Pa *and (b) 800* Pa*. Circles are the experimental data and solid line is the best fit.*

transform of a convolution of two (or more) functions is proportional to the product of the individual Fourier transforms. Consequently, the *fft*-transforms of the instrumental function, the Doppler function and the Lorentzian function are multiplied in the inverse space. The resulting function (which is the Fourier transform of their convolution) is inversely transformed by *ifft.m* routine [22]. The program then compares the shape of this function with the experimental line shape in the least squares sense. The data reduction procedure outlined above yields the Lorentzian widths of three oxygen lines for different argon pressures. Figures 8a-c show the dependence of the obtained Lorentzian line widths on argon pressure. The dependence is linear, with relatively large error bars for all three transitions. The same type of dependence of Lorentzian widths on foreign gas (here argon) pressure is predicted theoretically as [23]

$$\Delta\lambda_L^O = \Delta\lambda_0^O + C \cdot p_{Ar}. \tag{1}$$

Here $\Delta\lambda_0^O$ contains the contribution to the oxygen line width which is independent of gas pressure - the natural line width. The dependence of oxygen line width on argon pressure is contained in the $C \cdot p_{Ar}$ term, where p_{Ar} stands for argon pressure. The possible contribution of the oxygen self-broadening can be neglected because of the very low density of oxygen atoms caused by a low dissociation rate of molecular oxygen in Ar-O_2 plasmas [6,9]. Consequently, in our experimental conditions both these contributions to the total line width are negligible compared to the argon pressure broadening.

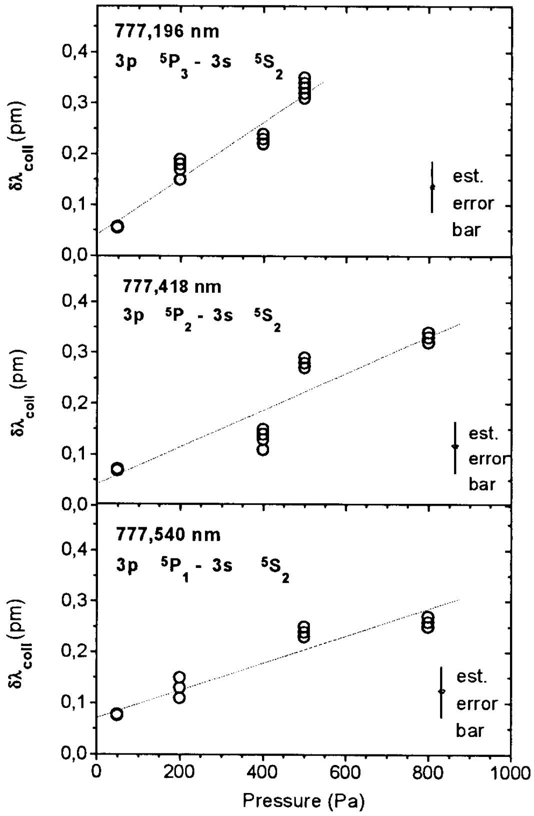

Fig. 8. Results for the collisional line widths versus gas pressure for oxygen transitions (a) $^5P_3 \rightarrow\ ^5S_2$, *(b)* $^5P_2 \rightarrow\ ^5S_2$, *(c)* $^5P_1 \rightarrow\ ^5S_2$. *Estimated average error bar for the determination of Lorentzian line widths is about 50%.*

The broadening parameter C is proportional to the optical cross-section for neutral broadening σ_R [19]. A comprehensive discussion and the compilation of the experimental pressure broadening and shift data for a number of atomic lines are given in Ref. 24. Our line widths are related to the Lewis' definition of the optical cross-section for neutral broadening, σ_R, via broadening parameter C

$$\Delta\lambda_L^O \approx C \cdot p_{Ar} = \frac{\lambda_0^2}{\pi c}\,\sigma_R\,\overline{v}\,\cdot N_{Ar} = \frac{\lambda_0^2\overline{v}}{\pi ckT}\sigma_R \cdot p_{Ar}, \tag{2}$$

where $\overline{v} = \sqrt{8kT/\pi\mu}$ represents the average atom velocity, λ_0 is the wavelength of the line centre and N_{Ar} is argon density. The symbols π, k, c and μ have their usual meaning.

TABLE 1. The broadening coefficients for three oxygen lines. The estimated average error is about 50%.

Transition	^{5}P$_3$ $\to$ ^{5}S$_2$	^{5}P$_2$ $\to$ ^{5}S$_2$	^{5}P$_1$ $\to$ ^{5}S$_2$
λ(nm)	777,196	777.418	777.540
$\Delta\lambda_L^0/p_{Ar}$ (10^{-4} pm/Pa)	6	4	3

The broadening parameters C for the three oxygen lines are given in Table 1. We estimate that the average error of the determination of Lorentzian line widths and resulting broadening parameters is about 50%. This estimate is based on the uncertainty in the measurement of the instrumental width, uncertainty in the determination of the Doppler width, on the average signal-to-noise ratio and on the maximal estimated error in the determination of the Lorentzian width using our fitting procedure. The major contribution to the large relative error comes from the fitting procedure we used for the determination of the collision line widths. The collision line width amounts about 15% (or less) of the total experimental line width and despite of the use of the sophisticated software for the numerical line shape analysis, the final number is inevitably determined with a large uncertainty. Particularly, due to the poorer signal-to-noise ratio, the relative error bar is even larger for the lowest pressures. To our knowledge there is so far no measurement of 777 nm oxygen line broadening reported in the literature and we have nothing to relate our results to. However, one can note that the data have similar order of magnitude as in the case of typical noble gas - noble gas line broadening experiments [25].

4. Conclusion

The electron temperature was determined using the double-probe technique and the logarithmic plot method. The electron temperatures of both the DC discharge and the RF discharge increase with the addition of oxygen. In pure argon, it is about 3 eV for DC excitation (1.7 eV for RF excitation), and in Ar+10%O$_2$ mixture and DC excitation it is about 3.3 eV (2.3 eV for RF excitation). In the case of the DC discharge, one can see a small decrease of the electron temperature with pressure.

We performed emission measurements of the line widths of oxygen lines at 777 nm (^{5}P$_{3,2,1}$ $\to$ ^{5}S$_2$) broadened by argon. Line profiles were measured with the high-resolution monochromator and later analyzed numerically. The obtained broadening coefficients have large error bars because of the indirect determination method. Further measurements of the broadening and, also, the shift coefficients using the Doppler-free high-resolution laser spectroscopy methods would be of great interest.

Acknowledgements

This research was supported by the grant JF107/NIST/Veza of the USA-Croatia Joint Fund for Cooperation in Science and Technology and by a joint project of the Germany-Croatia Bilateral Fund for Cooperation in Science (administered by KFA Juelich), and by the Ministry of Science and Technology of the Republic of Croatia.

References

1) J. Norman Bardsley, *International Conference on Atomic and Molecular Data and Their Applications*, W. Wiese ed., NIST (Gaithersburg, MD, USA) (1997);

2) S. Rauf and M. J. Kushner, J. Appl. Phys. **82** (1997) 2805;

3) T. R. Brumleve, *Proceedings of the 3rd International Symposium on the Science and Technology of Light Sources*, Tolouse (1983) 43:P; G. Zilberstein and H. J. Kim, *Proceedings of the 6th International Symposium on the Science and Technology of Light Sources*, Budapest (1992) 42:L;

4) A. Zybin, C. Schnürer-Patschan and K. Niemax, Spectrochim. Acta **B48** (1993) 1713;

5) D. Park, D. Lee, M. H. Kim, T. Park, H. Woo, E. Yoon, D. Chun and J. Ha, *MRS Conference Proceedings* (1996), (http://www.tycl.co.kr/papers/mrs200.htm);

6) Edith Konz, *Doktorarbeit*, Max-Planck-Institut für Strömungsforschung, Uni Göttingen (1996);

7) A. Catherinot, P. Placidet and B. Dubreuil, J. Phys. **B21** (1978) 3775;

8) W. P. West, T. B. Cook, F. B. Dunning, R. D. Rundel and R. F. Stebbings, J. Chem.Phys. **63** (1975) 1237;

9) A. Sasso, *Inst. Phys. Conf. Ser., Vol.113 (Int. Meeting on OGS-1990)*, Institute of Physics (1990) 169;

10) M. S. Feld, B. J. Feldman and A. Javan, Phys. Rev. **A7** (1973) 257;

11) N. Kwon, Y. Yun and W.Jhe, Phys. Rev. **A52** (1995) R895;

12) G. M. Tino, Comments At. Mol. Phys. **29** (1993) 5;

13) C. Sansonetti, private communication (1995);

14) I. Langmuir, General Electric Review **26** (1923) 731;

15) I. Langmuir and H. Mott-Smith, General Electric Review **27** (1924) 449;

16) E. O. Johnson, L. Malter, Phys. Rev. **80** (1950) 58;

17) V. Godyak, R. Piejak and B. Alexandrovich, *Phenomena in Ionized Gases XXII*, Hoboken, NJ (July 1995), eds. K. H. Becker, W. E. Carr and E. E. Kunhardt, AIP Press;

18) J. T. Gudmundsson, T. Kimura and M. A. Lieberman, *Gaseous Electronics Conference 1997*, paper JTP3.28, October 07, 1997, AIP Press (1997);

19) W. Demtröder, *Laser Spectroscopy* (Springer-Verlag Berlin, Heidelberg) Chapt. 3 (1981);

20) Jobin Yvon THR1500 Manual;

21) K. Tachibana, H. Harima and Y. Urano, J. Phys. **B15** (1982) 3169;

22) The Student Edition of "Matlab" (Ver. 4), Prentice Hall and The MathWorks Inc., Englewood Cliffs, NJ 07632 (1995);
The "Matlab" (even our student version) is a very powerful software package and computing environment used by many university laboratories and R&D laboratories of many leading companies. By our experience, it is by far the most powerful software for "number crunching" tasks and signal processing. See also http://www.mathworks.com;

23) A. Corney, *Atomic and Laser Spectroscopy* (Clarendon Press, Oxford) Chapt. 8 (1977);

24) E. L. Lewis, Physics Reports **58** (1980) 1;

25) A. Bielski, S. Brym, J. Szudy, R. S. Travinski and J. Wolnikowski, J. Phys. **B24** (1991) 4909.

EKSPERIMENTALNO PROUČAVANJE Ar–O_2 IZBOJA PRI NISKOM TLAKU

Izvješćujemo o mjerenjima elektronske temperature pri istosmjernom i radiofrekventnom izboju u čistom Ar i u plinskoj smjesi Ar + 10% O_2, i o mjerenjima sudarnog širenja argonom triju kisikovih linija na 777 nm (3p $^5P_{0,1,2} \rightarrow$ 3s $^5S_2$ prijelazi) u plinskoj smjesi Ar + 10% O_2. Elektronska se temperatura određivala pomoću dviju sondi i metodom logaritamskog dijagrama. Širine kisikovih linija su se mjerile pomoću monokromatora visokog razlučivanja te numerički analizirale.